JOURNAL OF MATERIALS SCIENCE 19 (1984) 3451–3458

Internal oxidation of Fe–Si alloys in γ-phase region

JUN TAKADA, KEN KASHIWAGI*, MASAO ADACHI
Department of Metal Science and Technology, Kyoto University, Sakyo-ku, Kyoto 606, Japan

Internal oxidation measurements of Fe–0.070, 0.219, 0.483, and 0.920 wt % Si alloys were made in the γ-phase region in order to discuss kinetics of internal oxidation, to evaluate the diffusion coefficient of oxygen in the internal oxidation layer, and to determine the diffusion coefficient of oxygen in γ-iron. Internal oxidation of these alloys was conducted at temperatures between 1223 and 1323 K using a powder mixture of iron and Fe_2O_3. The internal oxidation front in Fe–Si alloys with between 0.070 and 0.483 wt % Si advances in parallel to the specimen surface. The internal oxidation in these alloys obeys a parabolic rate law, which indicates that the internal oxidation is controlled by an oxygen diffusion process in the alloy. The diffusion coefficient of oxygen, D_O^{IO}, in the internal oxidation layer where SiO_2 particles disperse was determined by using the thermodynamic data for the solution of oxygen in γ-iron. D_O^{IO} increases with the increase of the volume fraction of the oxide, f^{IO}, in the oxidation layer at a given temperature. The diffusion coefficient of oxygen, D_O, in γ-iron was evaluated by extrapolating D_O^{IO} to $f^{IO} = 0$. D_O may be given by the following equation:

$$D_O = \left(6.42 \begin{matrix} +4.37 \\ -2.60 \end{matrix}\right) \times 10^{-5} \exp\left[-\frac{159 \pm 5 \text{ (kJ mol}^{-1})}{RT}\right] \text{m}^2 \text{ sec}^{-1}.$$

1. Introduction

Internal oxidation is the process by which oxygen diffuses into an alloy and forms the oxide of one or more alloying elements which must be less noble than the solvent metal. Internal oxidation is of interest and importance from a practical standpoint for a number of reasons. Internal oxidation provides a method of introducing second-phase particles into an alloy. Dispersion strengthened alloys obtained by this method have excellent mechanical properties [1, 2], and especially a superior elevated temperature strength [3, 4], because the dispersed phase formed in the alloy is oxide which is stable even at elevated temperatures. Internal oxidation measurements supply a great deal of basic information for the study of high temperature oxidation of alloys [5]. Moreover, internal oxidation measurements are used to evaluate the product of solubility and diffusion coefficient (permeability) for oxygen in the alloy [6–8]. In the case where the solubility of oxygen in the alloy is known, the diffusion coefficient of oxygen can be determined [9, 10].

The objects of the present work on the internal oxidation of Fe–Si alloys are as follows. The first is to find suitable conditions for the uniform distribution of second particles in the alloys. These conditions are required for dispersion strengthened alloys. Secondly, it is to study the process which controls the internal oxidation of these alloys. There have been few data [10] on the diffusion coefficient of oxygen in the internal oxidation layer of iron alloys, and those for γ-iron have not been investigated. The third purpose is, therefore, to evaluate the diffusion coefficient of oxygen in the internal oxidation layer and subsequently to

*Present address: Nippon Koshuha Steel Co., Let, Shinminato, Toyama 934, Japan.

0022–2461/84 $03.00 + .12

determine the diffusion coefficient of oxygen in γ-iron by extrapolation.

2. Materials and experimental procedure

Fe–0.070, 0.219, 0.483, and 0.920 wt % Si alloys were made by melting in vacuum. The alloys were swaged and cut to approximately $5 \times 5 \times 4\,mm^3$. The specimens were annealed in vacuum to yield similar grain sizes of about 40 μm. Chemical compositions of the alloys are shown in Table I. The surfaces of each specimen were mechanically polished with an abrasive paper of no. 1500. Then the specimens were internally oxidized by the pack method using a powder mixture, composed of 1 part iron, 1 part Fe_2O_3, and 1 part Al_2O_3 powders. The internal oxidation temperatures were 1223, 1273 and 1323 K, which were controlled within ± 3 K. Fe–0.920 wt % Si alloy was internally oxidized at 1373 K in addition to the above temperatures. Internally oxidized specimens were carefully cut parallel to their surface. The cross sections of the specimens were ground in the same way as described above and polished with diamond paste and then etched by 3% nital. The depth of the internal oxidation layer was measured using an optical microscope.

In order to determine the oxide formed in the internal oxidation layer the X-ray diffraction method was used. The oxide was carefully extracted from the oxidation layer by using the bromine–alcohol method and examined by X-ray diffraction using Co$K\alpha$ radiation. X-ray analysis was conducted under the following conditions: accelerating voltage, 30 kV; anode current, 30 mA; filter, iron.

The concentration profile of solute element, i.e. silicon in the internal oxidation specimen, was examined by an electron probe microanalyser (Hitachi X-650 type). The operating conditions of the microanalyser were as follows: accelerating voltage, 20 kV; take-off angle of radiation, 38° (0.66 rad); specimen current, 0.012 μA. The known silicon content of the alloys with no oxidation treatment and pure iron whose silicon content is less than 0.001 wt % was used as a calibration standard. The relationship between the relative intensity of X-ray and the silicon concentration was found to be linear.

TABLE I Chemical compositions of the alloys used (wt %)

Alloy	Si	C	Mn	P	S
Fe–0.070 Si	0.070	0.004	0.003	0.004	0.005
Fe–0.219 Si	0.219	0.005	0.003	0.003	0.005
Fe–0.483 Si	0.483	0.004	0.004	0.003	0.005
Fe–0.920 Si	0.920	0.004	0.003	0.003	0.005

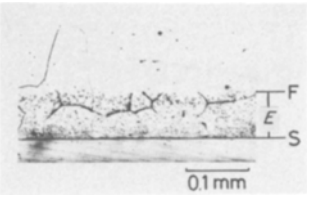

Figure 1 Micrograph showing the microstructure of Fe–0.219 wt % Si alloy internally oxidized for 32.4×10^3 sec at 1273 K. S and F indicate the specimen surface and the internal oxidation front, respectively. *E* shows the thickness of the internal oxidation layer.

3. Results

3.1. Features of internal oxidation layer

Typical microstructures of internally oxidized alloys are shown in Figs. 1 and 2. Fig. 1 shows a microstructure of Fe–0.219 wt % Si alloy internally oxidized at 1273 K for 32.4×10^3 sec. In this figure *E* indicates the thickness of the internal oxidation layer, that is, the distance between the specimen surface and the internal oxidation front. It is seen that the oxidation front is nearly parallel to the specimen surface. This type of internal oxidation layer is termed normal according to the classification of the internal oxidation layers formed in iron alloys [11]. Fig. 2 shows the microstructure of Fe–0.920 wt % Si alloy internally oxidized at 1373 K for 259×10^3 sec. The internal oxidation front in this alloy is not parallel to the specimen surface and the layer appears to consist

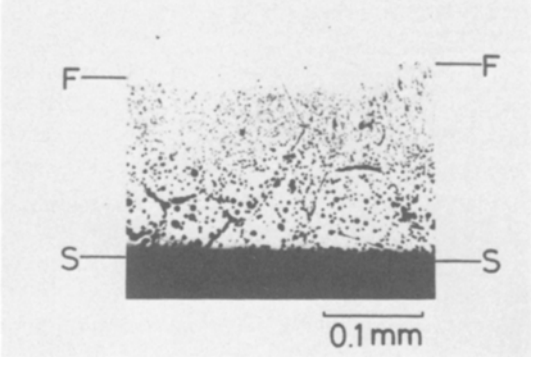

Figure 2 Micrograph showing the microstructure of Fe–0.920 wt % Si alloy internally oxidized for 259×10^3 sec at 1373 K. S and F indicate the specimen surface and the internal oxidation front, respectively.

of two regions: one is the region near the specimen surface in which large particles disperse, and the other is the inner region where small particles disperse. This type of oxidation layer was observed only in Fe–0.920 wt % Si alloy, while the normal type of oxidation layer as shown in Fig. 1 was observed in the other Fe–Si alloys. Similar abnormal types of oxidation layers are often formed in iron alloys of higher solute content [11, 12]. The data on Fe–0.920 wt % Si alloy were not used in the analysis of this work, because the thickness of the internal oxidation layer could not be accurately determined.

The oxide formed in internally oxidized Fe–Si alloys is expected to be SiO_2 or a complex oxide of iron and silicon, e.g. fayalite (Fe_2SiO_4). The oxide in the internal oxidation layer was extracted by the bromine–alcohol method and identified by X-ray diffraction. No reflections were observed. Ashby and Smith [13] have found that the oxide of silicon introduced into copper by the internal oxidation technique is amorphous SiO_2. These results suggest that the oxide formed in the internal oxidation layer of Fe–Si alloys may be amorphous SiO_2.

3.2. Relationship between thickness of the internal oxidation layer and oxidation time

Fig. 3 shows the relationship between the square of the thickness, E^2, of the internal oxidation layer and the oxidation time, t, for Fe–0.219 wt % Si alloy internally oxidized at 1223, 1273 and 1323 K. Fig. 4 shows the similar relationship

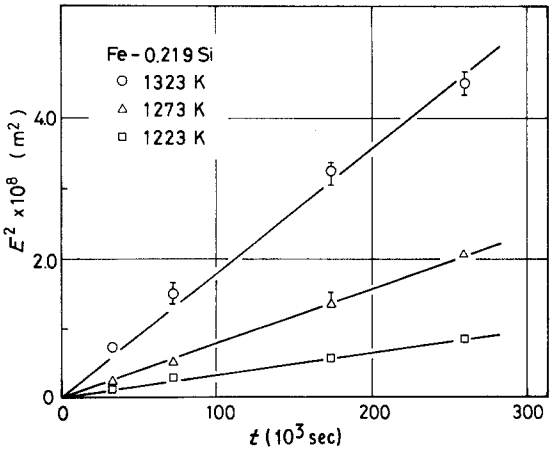

Figure 3 Relationship between the square of the thickness of the internal oxidation layer and the oxidation time for Fe–0.219 wt % Si alloy.

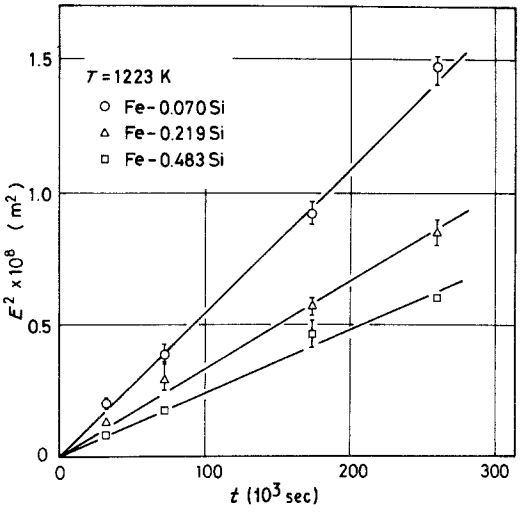

Figure 4 Relationship between the square of the thickness of the internal oxidation layer and the oxidation time for Fe–0.070, 0.219 and 0.483 wt % Si alloys internally oxidized at 1223 K.

for Fe–0.070, 0.219 and 0.483 wt % Si alloys internally oxidized at 1223 K. These results indicate that the relationship between E^2 and t can be expressed as

$$E^2 = K_p t, \tag{1}$$

where K_p is a constant at a given temperature for each alloy. Thus the internal oxidation process in these alloys obeys a parabolic rate law. As the constant K_p corresponds to the penetration rate of the internal oxidation front, K_p is called the rate constant. As shown in Figs. 3 and 4, K_p increases with the increase of the oxidation temperature and with the decrease of the content of the solute element. Fig. 5 indicates the temperature dependence of the rate constant K_p. Then K_p is given for each alloy by

$$K_p = K_p^* \exp\left(-\frac{Q_K}{RT}\right), \tag{2}$$

where K_p^* is a constant, R is the gas constant, T is the oxidation temperature and Q_K is the activation energy for the penetration of the internal oxidation front. Q_K can be calculated from the slope of the straight lines drawn in Fig. 5, and the values of Q_K are given Table II.

4. Discussion

4.1. Internal oxidation process

It is seen in Figs. 3 and 4 that the internal oxidation process in Fe–Si alloys except Fe–0.920 wt % Si

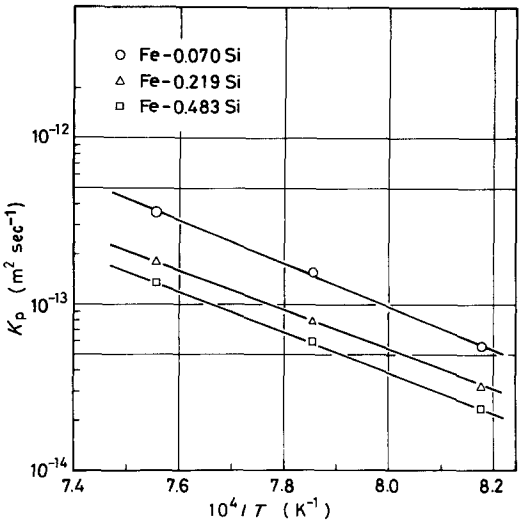

Figure 5 Temperature dependence of the rate constant, K_p.

alloy follows a parabolic rate law. This fact suggests that the internal oxidation in these alloys is controlled by a diffusion process of oxygen [14].

Theoretical treatments for kinetics of internal oxidation have been reported by several investigators [6, 15–17]. In the present work the case in which only an internal oxidation layer is formed is discussed, and it is assumed that in the internal oxidation process the following conditions are satisfied: the nucleation and growth of the oxide occur without any disturbance; at the oxidation front the solubility product of the oxide is so low that the concentration of the solute element is negligible. A parabolic rate constant, r, is defined as follows [15]:

$$r = \frac{E}{2(D_O^{IO}t)^{1/2}}, \tag{3}$$

where D_O^{IO} is the diffusion coefficient of oxygen in the internal oxidation layer, which should be distinct from the diffusion coefficient of oxygen in γ-iron. When $r \ll 1$, a relationship between the thickness of the internal oxidation layer and the oxidation time is given by [6, 15]

$$E^2 = \frac{2N_O^S D_O^{IO}}{\nu N_B} t F(z), \tag{4}$$

where

$$F(z) = \pi^{1/2} z \exp(z^2) \operatorname{erfc}(z) \tag{5}$$

and

$$z = \frac{E}{2(D_B t)^{1/2}}. \tag{6}$$

In these equations N_O^S is the concentration of dissolved oxygen at the specimen surface, N_B, is that of the solute element, B, in the bulk alloy, ν is the ratio of oxygen atoms to metal atoms in the oxide, and D_B is the diffusion coefficient of the solute element in the bulk alloy. For the limiting case when $z \gg 1$, $F(z)$ is approximately equal to 1. This reveals that the diffusion of the solute element from the bulk alloy to the oxidation front, that is, the counterdiffusion of B, is negligible as compared with that of oxygen from the specimen surface to the oxidation front. In the case where $F(z)$ is smaller than 1, the counterdiffusion of B cannot be neglected. In this case the internal oxidation layer is enriched with the solute element. The concentration of the solute element in the internal oxidation layer can be evaluated by $N_B/F(z)$, where $1/F(z)$ is called the enrichment factor, β [8, 16].

From Equations 4 to 6 one can determine the product of the solubility and the diffusion coefficient, $N_O^S D_O^{IO}$, for oxygen in the internal oxidation layer. This can be used to evaluate the penetration of oxygen in the high temperature oxidation of iron alloys in which N_O^S cannot be determined independently. When N_O^S is known, D_O^{IO} can be evaluated.

4.2. Oxygen concentration at the specimen surface

No direct measurements on the oxygen concentration, N_O^S, at the specimen surface in iron alloys internally oxidized by means of a powder mixture of iron and its oxide have yet been reported. The author [18] has found that the oxygen pressure at the outer surface of the specimen in the internal oxidation with a powder mixture in iron and Fe_2O_3 is equal to the equilibrium oxygen pressure of FeO. Therefore, using both the thermodynamic data [19] for this reaction and the data for the solution of oxygen in γ-iron [10], the concentration

TABLE II Values of the activation energy, Q_K, for the penetration of the internal oxidation front in Fe–Si alloys

	Fe–0.070 Si	Fe–0.219 Si	Fe–0.483 Si
Q_K (kJ mol^{-1})	252 ± 10	228 ± 1	236 ± 3

TABLE III Values of oxygen concentration, N_O^S, at the specimen surface

	T (K)		
	1223	1273	1323
N_O^S	1.10×10^{-5}	1.52×10^{-5}	2.06×10^{-5}

of the dissolved oxygen (%O) in weight per cent can be evaluated from the following equation:

$$\log (\%O) = -\frac{4414}{T} + 0.1071. \quad (7)$$

From Equation 7 one can calculate the oxygen concentration, N_O^S, at the specimen surface in iron alloys internally oxidized by using a powder mixture of iron and Fe_2O_3. The values of N_O^S calculated are given in Table III.

4.3. Concentration of the solute element in the internal oxidation layer

The concentration of silicon in the internal oxidation layer can be evaluated from $N_B/F(z)$ or βN_B as described in Section 4.1. By combining Equations 1 and 6, z can be determined by the following equation:

$$z = \frac{K_p}{2(D_{Si})^{1/2}}. \quad (8)$$

In the present investigation the following data [8] on the diffusion coefficient of silicon were used:

$$D_{Si} = 2.1 \times 10^{-5} \exp\left[-\frac{242 \text{ (kJ mol}^{-1})}{RT}\right] \text{m}^2 \text{ sec}^{-1}. \quad (9)$$

The values of z obtained are given in Table IV. Using these values, $F(z)$ and β were calculated from Equation 5, which are also shown in Table IV. In all Fe–Si alloys β is slightly higher than 1. This indicates that there is a little enrichment of silicon in the internal oxidation layer.

TABLE IV Values of z, $\beta = 1/F(z)$ and r which are given by Equations 8, 5 and 11, respectively

Alloy	T (K)	z	$\beta = 1/F(z)$	r
Fe–0.070 Si	1323	3.97	1.03	5.01×10^{-2}
	1273	4.24	1.03	4.32×10^{-2}
	1223	4.11	1.03	3.66×10^{-2}
Fe–0.219 Si	1323	3.28	1.04	2.86×10^{-2}
	1273	3.40	1.04	2.46×10^{-2}
	1223	3.33	1.04	2.09×10^{-2}
Fe–0.483 Si	1323	2.74	1.06	2.21×10^{-2}
	1273	2.50	1.07	1.89×10^{-2}
	1223	2.50	1.07	1.61×10^{-2}

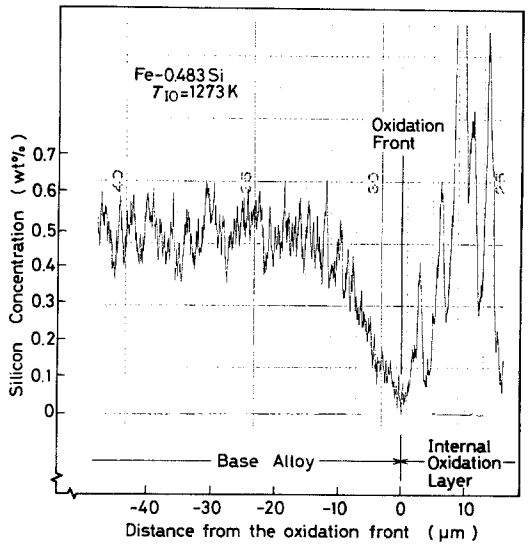

Figure 6 Concentration profile of silicon in Fe–0.483 wt % Si alloy internally oxidized at 1273 K.

To check whether β obtained from the above calculation is valid or not, the concentration profile of silicon in the internally oxidized specimen was investigated by an electron probe microanalyser. Fig. 6 shows the concentration profile of silicon in Fe–0.483 wt % Si alloy internally oxidized at 1273 K. It is seen that a little amount of silicon diffuses into the internal oxidation layer from the bulk alloy. The value of β determined in this alloy is 1.07 ± 0.03, which is in good agreement with the value of 1.07 obtained from the calculation using the diffusion coefficient of silicon. This result, therefore, suggests that the diffusion of silicon to the oxidation front from the bulk alloy is not negligible and β in Table IV is valid.

4.4. Diffusion coefficient of oxygen in the internal oxidation layer

Since the oxygen concentration at the specimen surface and the concentration of silicon in the internal oxidation layer have been determined, the diffusion coefficient of oxygen, D_O^{IO}, was evaluated from Equations 4 to 6. Fig. 7 shows the temperature dependence of D_O^{IO}. In each alloy D_O^{IO} may be expressed as

$$D_O^{IO} = A^{IO} \exp\left(-\frac{Q_O^{IO}}{RT}\right), \quad (10)$$

where A^{IO} is the frequency factor and Q_O^{IO} is the activation energy for diffusion of oxygen in the internal oxidation layer. The values of A^{IO} and

TABLE V Values of the frequency factor, A^{IO}, and the activation energy, Q_O^{IO}, for diffusion of oxygen in the internal layer of Fe–Si alloys

	Fe–0.070 Si	Fe–0.219 Si	Fe–0.483 Si
A^{IO} ($m^2\ sec^{-1}$)	1.50×10^{-4}	2.48×10^{-5}	7.01×10^{-5}
Q_O^{IO} ($kJ\ mol^{-1}$)	167 ± 10	143 ± 1	152 ± 5

Q_O^{IO} are summarized in Table V. The values of Q_O^{IO} in the present alloys are in good agreement with that obtained in Fe–0.1 wt % Al alloy [10]. Fig. 7 indicates that D_O^{IO} increases as the concentration of silicon increases at a given temperature.

It is necessary to evaluate r in Fe–Si alloys in order to check whether or not the condition of $r \ll 1$ is satisfied. When $r \ll 1$, Equation 4 is valid as the rate equation of the internal oxidation in the present alloys. By combining Equations 1 and 3, r can be given by

$$r = \frac{1}{2}\left(\frac{K_p}{D_O^{IO}}\right). \quad (11)$$

The values of r computed from this equation by using the data of K_p and D_O^{IO} are given in Table IV. These values are smaller than 1. It is, therefore, clear that Equation 4 is valid in the present Fe–Si alloys.

4.5. Diffusion coefficient of oxygen in γ-iron

As shown Fig. 7, the diffusion coefficient of oxygen in the internal oxidation layer, where the oxide particles disperse, increases with the increase of the silicon content. This fact indicates that the existence of the oxide accelerates the diffusion of oxygen in γ-iron and D_O^{IO} depends on the content of the oxide in the internal oxidation layer. Then in Fig. 8 D_O^{IO} at each oxidation temperature is plotted as a function of the volume fraction of the oxide, f^{IO}, in the internal oxidation layer. f^{IO} was calculated from the silicon concentration in the oxidation layer which is given by βN_B. It is seen in Fig. 8 that the relationship between D_O^{IO} and f^{IO} is linear at each oxidation temperature. It can be expressed as

$$D_O^{IO} = D_O + b f^{IO}, \quad (12)$$

where D_O and b are constants. A similar relationship has been found in the previous investigations on Ni–Al and Ni–Cr alloys [9]. D_O^{IO} is controlled by the diffusion of oxygen not only in the matrix metal but also at the interface of the oxide and the matrix metal. As the content of the oxide increases, the former diffusion would decrease, while the latter would increase. In the case where the content of the oxide is small, the effect of the diffusion of oxygen in the matrix metal would be much smaller than that of the diffusion at the interface. Hence, D_O^{IO} would increase with the increase in f^{IO}. D_O is the diffusion coefficient of oxygen in the matrix metal where no oxide particles exist, i.e. γ-iron.

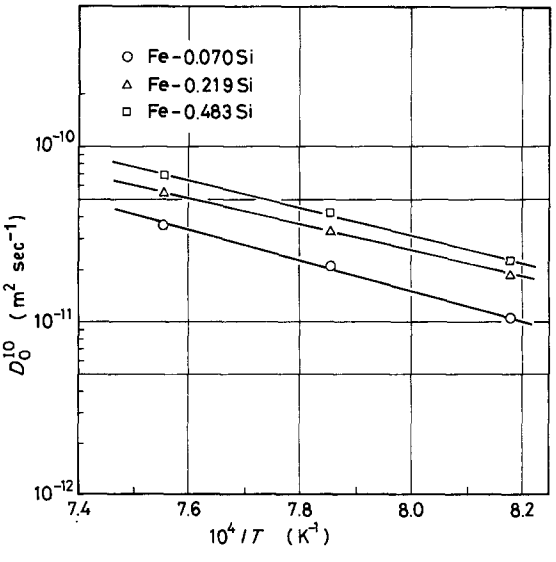

Figure 7 Temperature dependence of the diffusion coefficient of oxygen, D_O^{IO}, in the internal oxidation layer.

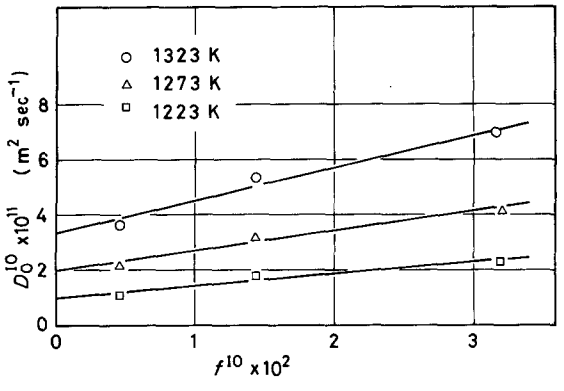

Figure 8 Relationship between the diffusion coefficient of oxygen, D_O^{IO}, and the volume fraction of the oxide, f^{IO}, in the internal oxidation layer.

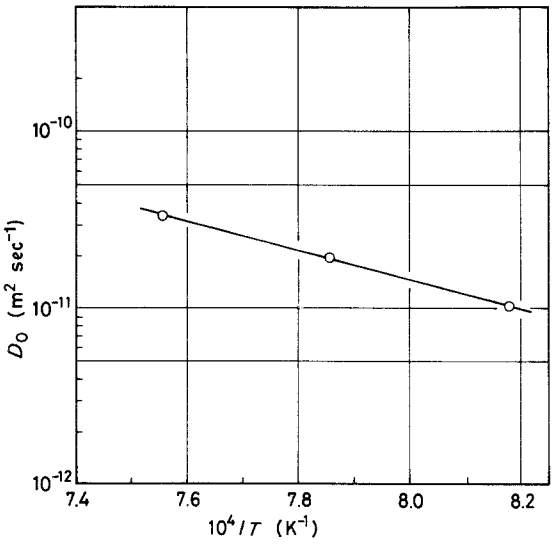

Figure 9 Temperature dependence of the diffusion coefficient of oxygen, D_O, in γ iron.

D_O was determined by extrapolating D_O^{IO} to $f^{IO} = 0$ according to Equation 12. The temperature dependence of D_O calculated is shown in Fig. 9. D_O may be expressed by the following equation:

$$D_O = A \exp\left(-\frac{Q_O}{RT}\right), \qquad (13)$$

where A is the frequency factor and Q_O is the activation energy for diffusion of oxygen in γ-iron. These values are given by

$$A = \left(6.42 \begin{matrix} +4.37 \\ -2.60 \end{matrix}\right) \times 10^{-5}\ m^2\ sec^{-1} \qquad (14)$$

and

$$Q_O = 159 \pm 5\ kJ\ mol^{-1}.$$

The interval of A and Q values represents the standard deviation which was calculated from the error variance of a linear regression of an Arrhenius plot of $\ln D_O$ against $1/T$.

5. Conclusion

Internal oxidation of Fe–0.070, 0.219, 0.483, and 0.920 wt % Si alloys was investigated for the purpose of obtaining information on the diffusion behaviour of oxygen in the γ-phase region. Internal oxidation was carried out in the temperature range 1223 and 1323 K using a powder mixture of iron and Fe_2O_3. The main results are:

1. in the alloys containing between 0.070 and 0.483 wt % Si the internal oxidation front penetrates parallel to the specimen surface with the oxidation time. In the oxidation layer of Fe–0.920 wt % Si alloy, the oxidation front is irregular;

2. the square of the thickness of the internal oxidation layer is proportional to the oxidation time. The proportional constant, namely the rate constant K_p, depends on silicon content in the alloys and oxidation temperature;

3. the oxygen concentration, N_O^S, at the specimen surface is evaluated by using the thermodynamic data for the solution of oxygen in γ-iron;

4. the internal oxidation layer is enriched with the solute element, i.e. silicon, because the diffusion of silicon to the oxidation front from the bulk alloy is not negligible;

5. the diffusion coefficient of oxygen, D_O^{IO} in the internal oxidation layer was calculated from the values of K_p, N_O^S, and the diffusion coefficient of silicon. D_O^{IO} increases with the increase in the volume fraction of the oxide, f^{IO}, in the internal oxidation layer;

6. the diffusion coefficient of oxygen, D_O, in γ-iron was determined by extrapolation of D_O^{IO} to $f^{IO} = 0$. D_O may be expressed as:

$$D_O = \left(6.42 \begin{matrix} +4.37 \\ -2.60 \end{matrix}\right) \times 10^{-5} \exp\left[-\frac{159 \pm 5\ (kJ\ mol^{-1})}{RT}\right] m^2\ sec^{-1}.$$

Acknowledgements

The authors are grateful to Dr Z. Asaki for helpful suggestions, K. Kimura for the X-ray diffraction work, T. Unezaki for the EPMA work, and T. Kitamura for his assistance in carrying out the experiments. Grateful acknowledgement is also made to the members of Center Research Laboratory, Kobe Steel, Ltd for melting of the alloys and chemical analysis, and Technical Research Center, Nippon Kokan K.K. for the extraction of the oxide.

References

1. R. EBELING and M. F. ASHBY, *Phil. Mag.* 13 (1966) 805.
2. J. TAKADA, K. KOYAMA and M. ADACHI, *J. Japan Inst. Metals* 42 (1978) 357.
3. B. A. WILCOX and A. H. CLAUER, *Trans. AIME* 236 (1966) 570.
4. J. TAKADA, S. MIYAWAKI, K. KAMATA and M. ADACHI, *J. Japan Inst. Metals* 47 (1983) 166.
5. H. NAGAI, T. MURAI and H. MITANI, *Trans. JIM* 20 (1979) 299.

6. J. PÖTSCHKE, P. M. MATHEW and M. G. FROHBERG, *Z. Metallkde* **61** (1970) 152.
7. M. T. HEPWORTH, R. P. SMITH and E. T. TURKDORGAN, *Trans. AIME* **236** (1966) 1278.
8. K. BOHNENKAMP and H. J. ENGELL, *Arch. Eisenhüttenw.* **35** (1964) 1011.
9. S. GOTO and N. KODA, *J. Japan Inst. Metals* **34** (1970) 319.
10. J. H. SWISHER and E. T. TURKDORGAN, *Trans. AIME* **239** (1967) 426.
11. Y. MIYOSHI and S. KADO, *J. Japan Inst. Metals* **31** (1976) 481.
12. R. WARD, *Trans. AIME* **162** (1945) 141.
13. M. F. ASHBY and G. C. SMITH, *J. Inst. Metals* **91** (1963) 182.
14. S. GOTO, K. NOMAKI and N. KODA, *J. Japan Inst. Metals* **31** (1967) 600.
15. C. WAGNER, *Z. Elektrochem.* **63** (1959) 772.
16. F. MAAK, *Z. Metallkde* **52** (1961) 545.
17. G. BÖHM and M. KAHLWEIT, *Acta Metall.* **12** (1964) 641.
18. J. TAKADA, Doctoral dissertation, Kyoto University (1982).
19. F. D. RICHARDSON and J. H. E. JEFFES, *J. Iron Steel Inst.* **160** (1948) 261.

Received 16 January
and accepted 24 January 1984